Iranian Journal of Science & Technology, Transaction A, Vol. 31, No. A4
Printed in The Islamic Republic of Iran, 2007

PREDICTION ALGORITHM FOR TORQUE RIPPLE REDUCTION IN DTC-BASED DRIVES*

SH. KABOLI[1**], M. R. ZOLGHADRI[1], P. ESKANDARI[1] AND D. ROYE[2]

[1]Electrical Engineering Department, Sharif University of Technology, Tehran, I. R. of Iran
[2]Polytechnic Institute of Grenoble, France
Email: kaboli@sharif.edu

Abstract – In direct torque control, the selection of an applied voltage vector is based on the measured parameters at the beginning of the sampling period. The delay between the measurement and the application of the voltage vector is the origin of an extra torque ripple. In this paper, a new predictive controller is proposed for compensating this delay and reducing the torque ripple. The stator current is measured twice in each sampling period and its expected value at the end of the period is predicted according to a linear extrapolation algorithm. Therefore, none of the machine parameters are used in the prediction, and consequently, the algorithm is quite robust against machine parameter variations. The calculation of the electromagnetic torque is performed using the predicted value of the stator current. Therefore, the selection of the voltage vector is more realistic and prevents extra torque ripple. This controller is quite suitable for high power drives where the sampling frequency is low, and there is enough time for the extra measurements. Simulation and experimental results which confirm the ability of this method to considerably reduce the torque ripple are presented.

Keywords – Induction motor drive, direct torque control, torque ripple, predictive controller

1. INTRODUCTION

Since the first development of the Direct Torque Control (DTC) concept [1-2], it has been used in many ac drive applications [3]. This is thanks to its simple structure, fast torque response and robustness against machine parameter variations. However, a direct torque controlled motor suffers from great torque ripples due to the fast response of the torque. The flux and electromagnetic torque of a motor are usually calculated using the measured stator current and voltage in a digital signal processor (DSP) to select the proper voltage vector that should be applied to the motor by an inverter. The voltage vector is constant during the sampling interval, while the current varies. Due to the digital nature of the DTC control loop, there is a time delay between the current and the voltage measurement for the calculation of the flux, torque and application of the voltage vector. In fact, the calculation of the torque and the selection of voltage vectors are based on measurements at the beginning of the sampling period. This delay leads to an extra torque ripple.

Some modified controllers have been proposed to reduce the torque ripple in DTC using prediction algorithms [4-9]. The method in [4-7] is based on space vector modulation and uses a prediction algorithm to determine the duty ratio of the voltage vectors in the next sampling period. This goal is achieved using the slope of the torque [4] or machine equations to calculate the torque [5-7]. All of these algorithms need to use machine equations and some parameters like rotor time constant. In [8], an energy function is defined and the behavior of the torque is evaluated for the next sampling period. But, its prediction

*Received by the editor December 31, 2005 and in final revised form January 2, 2008
**Corresponding author

algorithm is complex, and hence, computation time is increased. In [9], the prediction algorithm calculates the angle of the flux vector and selects a voltage vector with a minimum angle with respect to the flux vector. However, this method yields small improvements in the torque ripple.

Similar methods have been used to modify DTC in multi-level inverter drives [10] and its application for other motor types [11-12]. However, the above mentioned drawbacks exist for them too.

The method proposed in this paper uses a predictive controller designed for evaluating the motor torque at the end of a sampling period. It is shown that the fast dynamic of the stator current results in the fast torque response. In each sampling interval, the slope of the stator current is almost constant and can be calculated based on two measurements, one at the beginning of the sampling period and one with a sufficient delay within the same sampling. Therefore, the expected value of the stator current at the end of a sampling interval can be calculated through an extrapolation algorithm. Then, the predicted value of the torque is obtained using the expected value of the stator current at the end of the sampling period. Therefore, there is no need to use machine equations, and consequently, the method is insensitive to the variation of machine parameters. This method is quite suitable for high power drives, where the sampling period is long enough to provide enough time for a second current measurement and the consequent calculations. The results shown in this paper mainly deal with the compensation of the DTC delay. However, the advantages of the proposed method are not limited to this case and can be used with other torque ripple minimizing methods as well.

In the following sections, a brief introduction to the DTC of induction motors is presented. The effect of control loop delay on the motor torque ripple is explained, and then the proposed predictive controller is presented. Simulation and experimental results which justify the performance of the proposed controller are also presented.

2. DIRECT TORQUE CONTROL

A block diagram of DTC is shown in Fig. 1. The basic idea is to choose the best voltage vector, which makes the flux rotate and produce the desired torque. During this rotation, the amplitude of the flux remains within a pre-defined band. A two-level, three-phase voltage source inverter has six non-zero voltage vectors and two zero voltage vectors as shown in Fig. 2. Voltage vectors can be expressed:

$$\mathbf{U_i} = V_{dc} e^{j(i-1)\frac{\pi}{3}} \quad , i=1 \text{ to } 6 \tag{1}$$

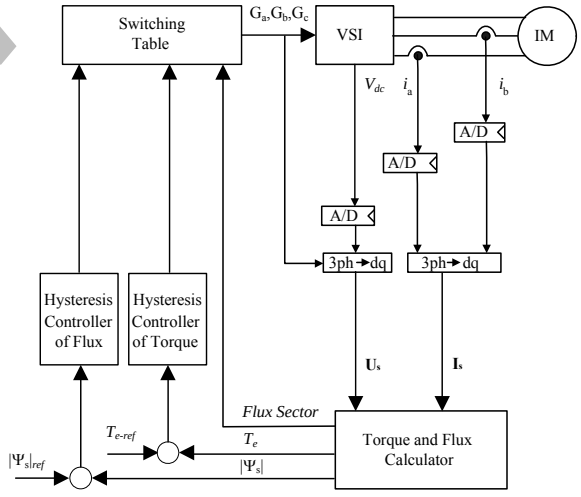

Fig. 1. Block diagram of the DTC method

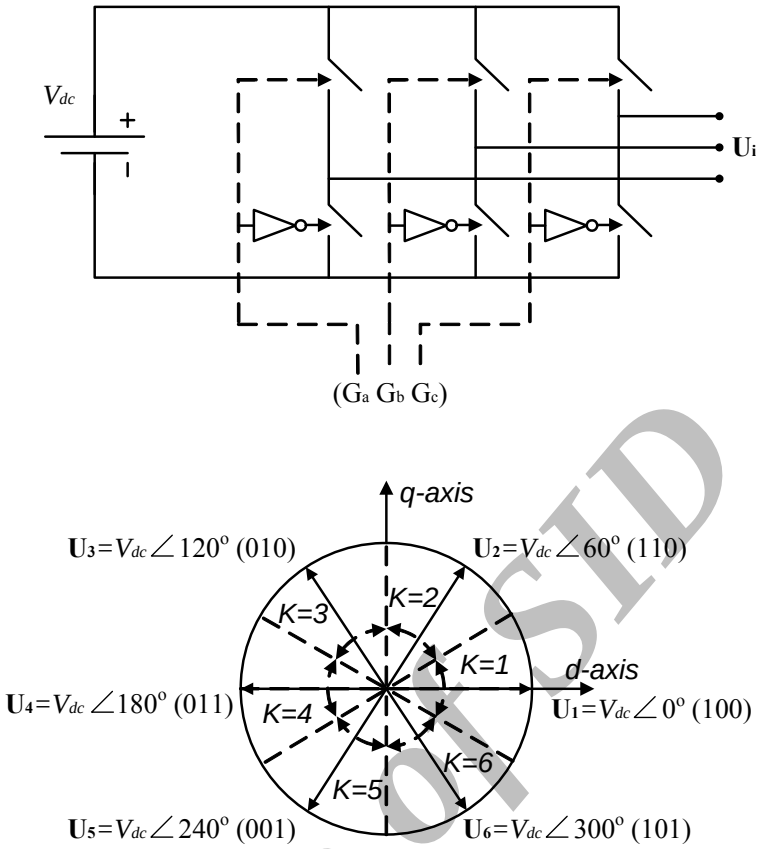

Fig. 2. Two-level three-phase inverter and its voltage vectors

Where j is the square root of -1. The stator flux vector can be calculated using the measured current and voltage vectors:

$$\frac{d\tilde{\boldsymbol{\psi}}_{\mathbf{s}}}{dt} = \mathbf{U}_{\mathbf{s}} - R_s \mathbf{I}_{\mathbf{s}} \tag{2}$$

or

$$\tilde{\boldsymbol{\psi}}_{\mathbf{s}} = \int (\mathbf{U}_{\mathbf{s}} - R_s \mathbf{I}_{\mathbf{s}}) dt \tag{3}$$

Then, the torque can be calculated using the components of the estimated flux and measured currents:

$$\tilde{T}_e = pp(\tilde{\psi}_{sd} I_{sq} - \tilde{\psi}_{sq} I_{sd}) \tag{4}$$

This relation is another presentation of the original torque equation (5) [1].

$$T_e = P \frac{L_m}{\sigma L_s L_r} |\boldsymbol{\psi}_{\mathbf{s}}| |\boldsymbol{\psi}_{\mathbf{r}}| \sin(\angle \boldsymbol{\psi}_{\mathbf{s}}, \boldsymbol{\psi}_{\mathbf{r}}) \tag{5}$$

Circular trajectory of the stator flux is divided into six symmetrical sectors referred to as the inverter voltage vectors, shown in Fig. 2. For each section, based on the torque and flux errors, a proper vector set is proposed. Four different switching methods are proposed for DTC which are shown in Table 1 [3]. Switching method A is the most usual one and is used in this study. The proposed method is independent of the switching methods.

Table 1. DTC switching strategies

	$T_e\uparrow \ \lvert\overline{\psi}_s\rvert\uparrow$	$T_e\uparrow \ \lvert\overline{\psi}_s\rvert\downarrow$	$T_e\downarrow \ \lvert\overline{\psi}_s\rvert\uparrow$	$T_e\downarrow \ \lvert\overline{\psi}_s\rvert\downarrow$
Solution A	U_{k+1}	U_{k+2}	U_8, U_7	U_8, U_7
Solution B	U_{k+1}	U_{k+2}	U_k	U_8, U_7
Solution C	U_{k+1}	U_{k+2}	U_k	U_{k+3}
Solution D	U_{k+1}	U_{k+2}	U_{k-1}	U_{k-2}

3. EFFECT OF CONTROL LOOP DELAY ON THE TORQUE RIPPLE

Sequential order of the tasks in a conventional DTC algorithm and some typical waveforms are shown in Figs. 3 and 4 respectively. The stator current is measured at the beginning of a sampling period ($I_{sa}(t_m)$ and $I_{sb}(t_m)$). Components of stator current ($I_{sd}(t_m)$ and $I_{sq}(t_m)$) and stator flux ($\psi_{sd}(t_{cf})$ and $\psi_{sq}(t_{cf})$) are calculated using the measured values and the torque is calculated ($T_e(t_{cT})$). The voltage vector is selected based on these calculations and is applied at the beginning of the next sampling period. A subinterval of no-operation (NOP) (T_{f1}) may exist, especially in high power drives where the switching frequency is low. Therefore, the voltage vector applied at the beginning of the next sampling period is based on the estimated torque and flux values which use the stator current measured at the beginning of the previous sampling period. Although the voltage vector applied is constant during one sampling interval, the stator current varies. This variation is the origin of the difference between the estimated torque and flux values and those of the motor. As shown in Fig. 4, the calculated torque $\widetilde{T}_e(t_{cT})$ is different from the real torque at that time ($T_e(t_{cT})$) and the error is more important at the end of the sampling period ($T_e(t+T_s)$) as E_T.

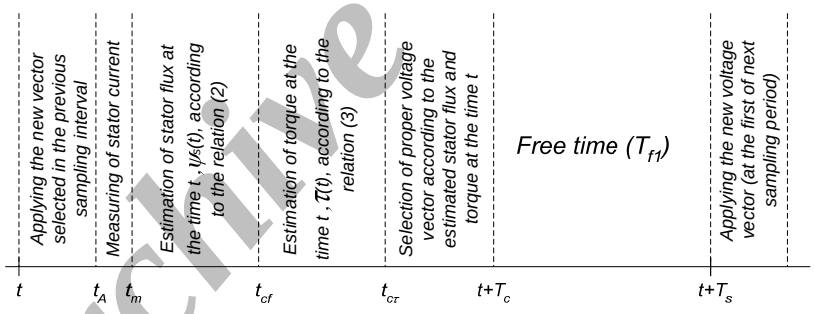

Fig. 3. Time diagram of conventional DTC

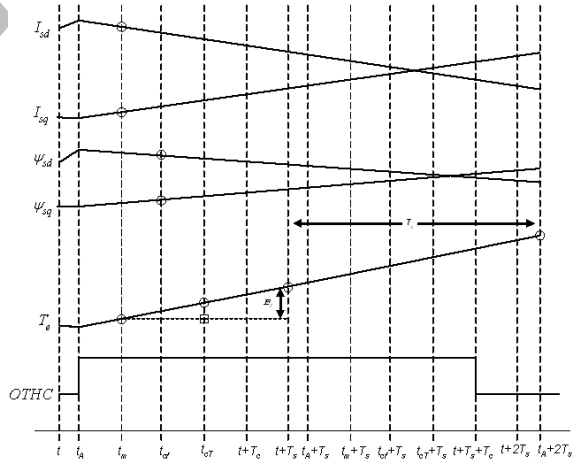

Fig. 4. Typical waveforms of motor parameters in conventional DTC

On the other hand, applying a forward rotating (/zero) voltage vector causes a great jump of motor torque at low (/high) speed because of the fast torque response of DTC. When the motor torque jumps out of the hysteresis band during a sampling interval, the DSP may not detect it in the same period. Therefore, the DSP continues to apply the incorrect vector in the next sampling time. Application of the incorrect voltage vector is the origin of an extra torque ripple.

4. PROPOSED PREDICTIVE CONTROLLER

The dynamic behavior of an induction machine described by the Eq. (6) to (9) written in terms of space vectors in a stator reference frame having a space vector model is shown in Fig. 5.

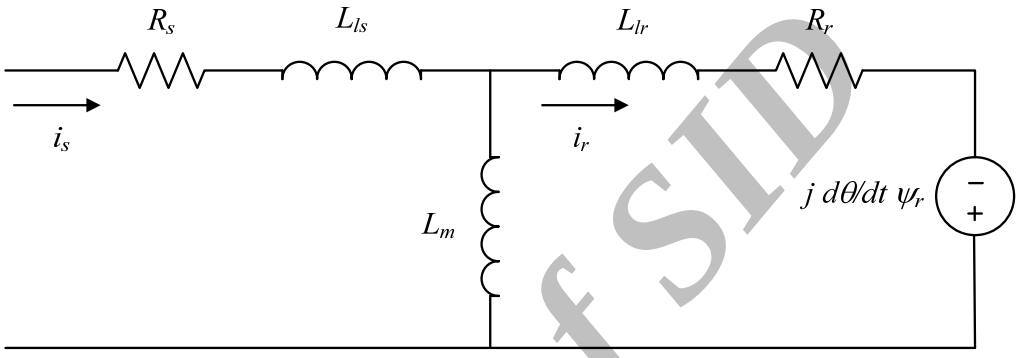

Fig. 5. Vector model of induction motor

$$\mathbf{V_s} = R_s \mathbf{I_s} + \frac{d\boldsymbol{\psi}_\mathbf{s}}{dt} \tag{6}$$

$$0 = R_r \mathbf{I_r} + \frac{d\boldsymbol{\psi}_\mathbf{r}}{dt} - j\omega\boldsymbol{\psi}_\mathbf{r} \tag{7}$$

$$\boldsymbol{\psi}_\mathbf{s} = L_s \mathbf{I_s} + L_m \mathbf{I_r} \tag{8}$$

$$\boldsymbol{\psi}_\mathbf{r} = L_r \mathbf{I_r} + L_m \mathbf{I_s} \tag{9}$$

After applying the derivative operator to Eq. (8) and (9), they can be rewritten as:

$$\frac{d\boldsymbol{\psi}_\mathbf{s}}{dt} = L_s \frac{d\mathbf{I_s}}{dt} + L_m \frac{d\mathbf{I_r}}{dt} \tag{10}$$

$$\frac{d\boldsymbol{\psi}_\mathbf{r}}{dt} = L_r \frac{d\mathbf{I_r}}{dt} + L_m \frac{d\mathbf{I_s}}{dt} \tag{11}$$

The time constant of the rotor flux is usually large and the rotor flux has a small variation during the sampling period [6]. Thus, the left hand side of Eq. (11) is equal to zero, and the variation of the stator current can be expressed according to the variation of the stator flux as follows:

$$\frac{d\mathbf{I_s}}{dt} = \frac{\dfrac{d\boldsymbol{\psi}_\mathbf{s}}{dt}}{\left(L_s - \dfrac{L_m^2}{L_r}\right)}$$

$$= \frac{\mathbf{V_s} - R_s \mathbf{I_s}}{\sigma L_s} \tag{12}$$

At normal operating points, when V_s is a non-zero voltage vector, $V_s >> R_s I_s$. Therefore, the slope of the stator current is almost constant during a sampling interval. Therefore, the basic control method based on the prediction of the torque can be presented as shown in Fig. 6a. with a time diagram. In the beginning of each sampling interval, the stator current is measured two times with a specific predefined delay between these two measurements. Assuming a linear variation for the current during a sampling interval, the expected value of the stator current in the end of a period can be extrapolated by (13):

$$\hat{I}_{\mathbf{s}}(t_1 + T_s) = \frac{d\mathbf{I_s}}{dt} T_s + \mathbf{I_s}(t_1)$$

$$= \frac{\mathbf{I_s}(t_{m2}) - \mathbf{I_s}(t_{m1})}{t_{m2} - t_{m1}} (T_s - t_{m2}) + \mathbf{I_s}(t_{m1}) \tag{13}$$

This prediction algorithm can be better simplified. Using Eq. (6), since the voltage effect on the flux variation is more important, using a measured stator current value instead of predicted values does not generate significant error in the estimated flux. Thus, flux estimation calculations can be done before the NOP interval between the first and second stator current measurements. This summarized prediction method is explained in Fig. 6b. It can be seen that the NOP interval between stator current measurements has been removed and the time interval needed for the flux calculation plays the role of this NOP interval.

Having the predicted value of the current at the end of a sampling time, the predicted value of the electromagnetic torque is calculated according to the predicted value of the stator current. And finally, the selection of the voltage vector is performed using the predicted value of the torque. It is assumed that the DC input voltage of the inverter is constant during the sampling time.

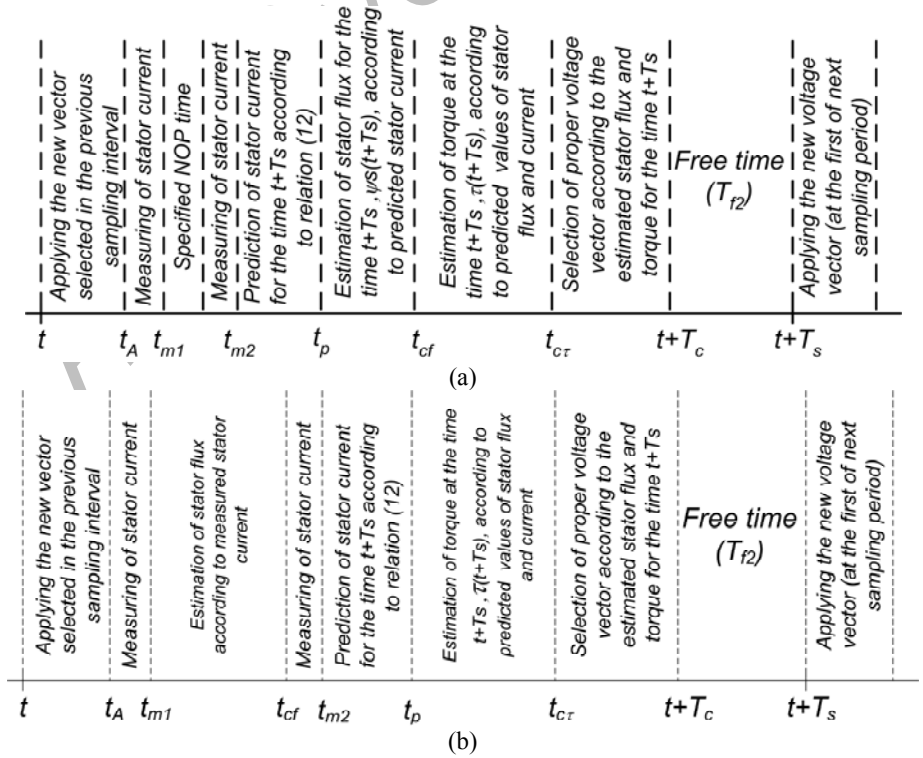

Fig. 6. Time diagram of modified DTC, (a): Basic control algorithm, (b): Summarized control algorithm

5. SIMULATION RESULTS

The parameters of the induction motor used in this study are shown in Table 2. The sampling period and the set point of the motor torque are 133 μsec and 10 N.m, respectively. The torque ripple factor in Eq. 14 is used for evaluating the quality of the torque ripple [13].

$$\delta = \sqrt{\frac{1}{T}\int_0^T \left(\frac{T_e}{T_{e-av}} - 1\right)^2 dt} \tag{14}$$

where T is the fundamental period of torque ripple.

Table 2. Characteristics of induction motor

Parameter	Value
Rated Power (KW)	5.5
Number of Poles	4
Stator Resistance (Ω)	0.18
Stator Inductance (mH)	56
Magnetizing Inductance (mH)	53
Rotor Resistance (Ω)	0.50
Rotor Inductance (mH)	56
Nominal Torque (N.m)	35
Nominal Stator Flux (Wb)	0.65

In the first simulation, the operation of conventional DTC and the proposed predicting method are compared to show the advantage of the proposed method. Fig. 7a shows the stator current used in the calculations. In the conventional DTC, the stator current used for torque calculation is measured at the beginning of the sampling interval and is considered constant during this interval. It can be seen that the stator current used for calculations is different from its real value at the end of the sampling interval. This difference acts like a time delay between the real stator current and its stored value at the end of the sampling period in the conventional DTC. This delay is more important when the stator current variation is high, while in the same Figure, it can be seen that using the predicting method, the values of the predicted stator current follow its real value at the end of a sampling interval.

Figure 7b shows this comparison between the estimated torque values in two methods. It can be seen that the predicted torque follows the actual torque, but there is a delay between the torque and its estimated value at the end of the sampling period in a conventional DTC.

In the second group of simulations, the DTC algorithm, once with the conventional estimation method and then with the prediction technique, is applied to the induction motor. Figures 8a and 8b show the steady state torque response of the machine at low speed (100 RPM) and high speed (1300 RPM) in the conventional DTC. When the output of the hysteresis torque controller (OHTC) commands to decrease or increase the torque, the torque is followed with a time delay. This leads to a great positive (/negative) torque ripple at low (/high) speed. The values of the torque ripple factor for low and high speed is 38% and 36%, respectively. Figures 8c and 8d show the results of using the application of the predictive controller. In this case, there is no delay between the torque controller and the torque. In fact, elimination of this delay is the main reason for torque quality improvement. For this case, the value of the torque ripple factor is 19% at low speed and 22% at high speed.

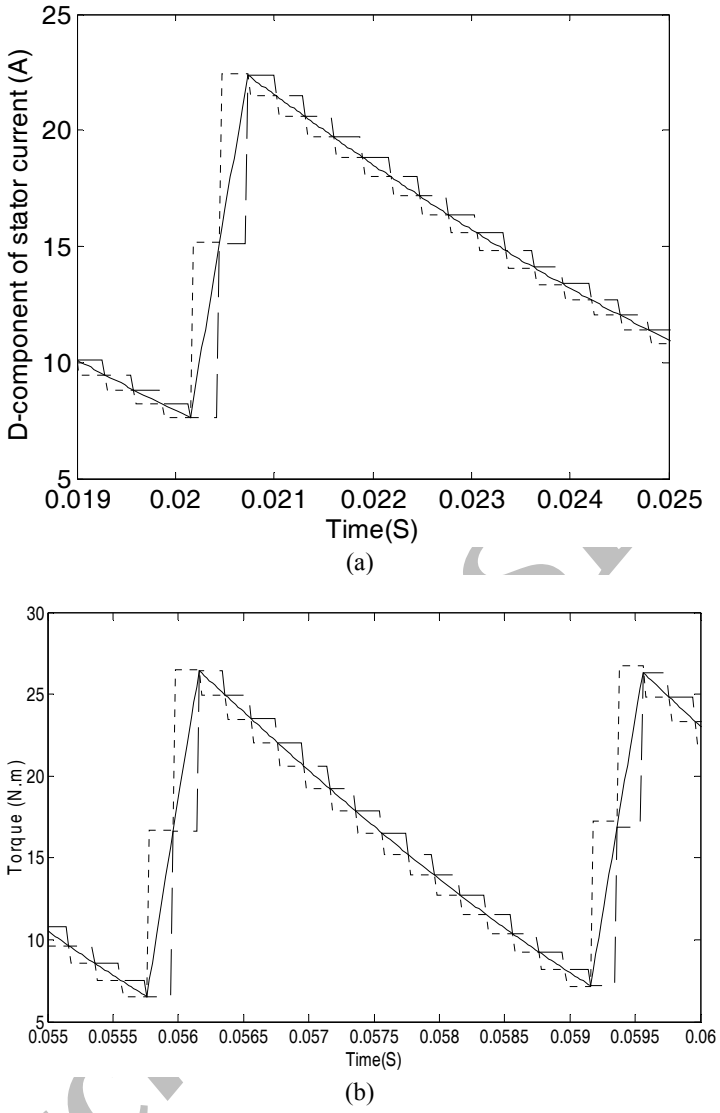

Fig. 7. Comparison between estimation of motor parameters in conventional DTC and proposed method, solid line: real value, dashed line: estimated or measured in conventional DTC, dotted line: predicted value in proposed method (a). d-component of stator current, (b). Torque

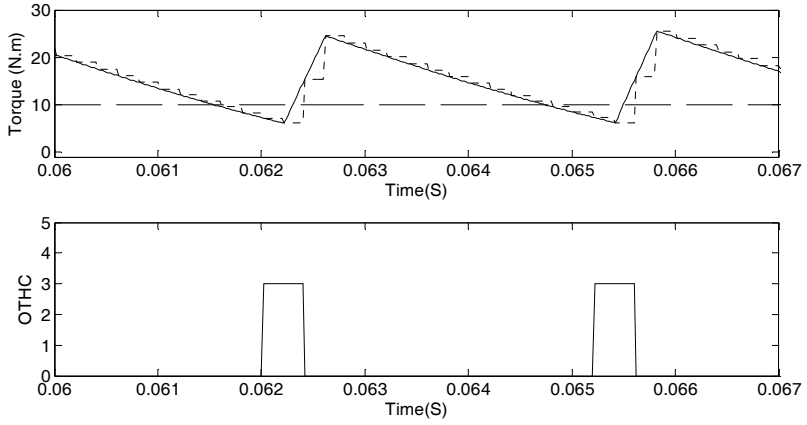

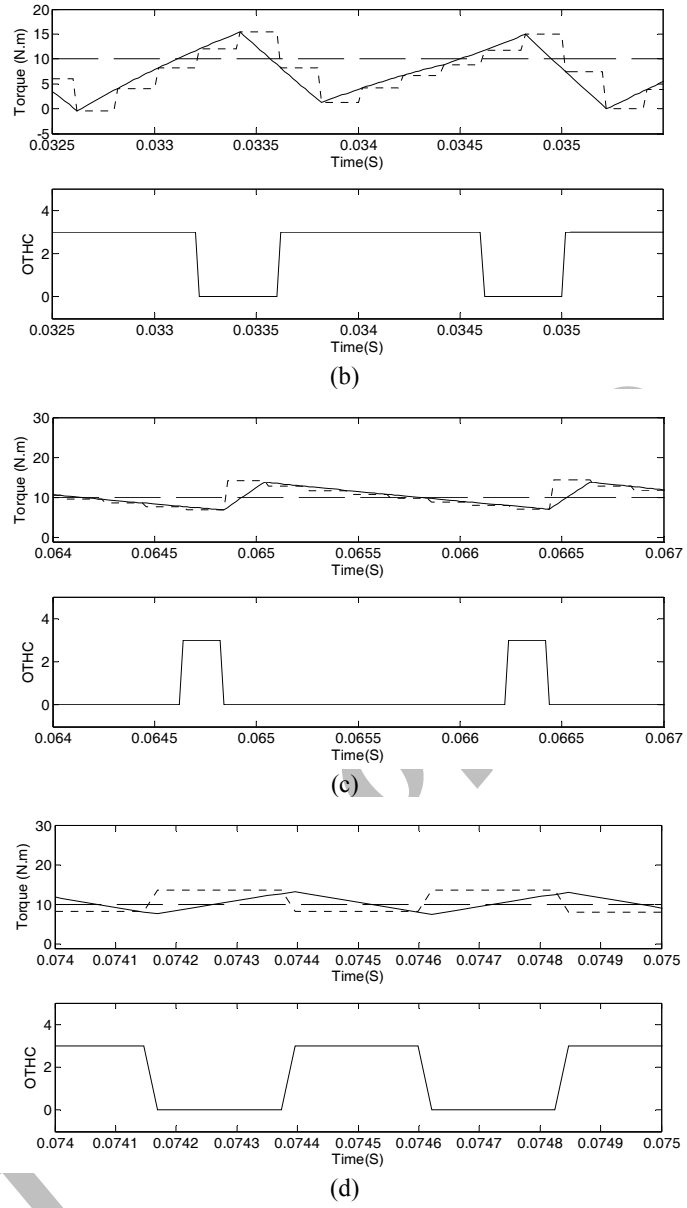

Fig. 8. Comparison between conventional DTC and proposed method, Up: torque response, solid line: real torque value, dashed line: reference torque, dotted line: estimated or predicted torque value Down: output of hysteresis torque controller
(a). low speed operation of conventional DTC
(b). low speed operation of modified DTC
(c). high speed operation of conventional DTC
(d). high speed operation of modified DTC

6. EXPERIMENTAL RESULTS

To verify computer simulation results, a DTC experimental test setup is implemented. The experimental setup, shown in Fig. 9, consists of an induction motor, insulated gate bipolar transistor (IGBT) based inverter, and a digital signal processor (DSP) based controller. Detailed characteristics of the inverter switches and DSP are presented in Table 3. The induction motor has the same characteristics as in the simulation. The machine currents i_a and i_b and the dc bus voltage were interfaced into the controller

through an analog to digital (A/D) converter built into the DSP board. The DSP board is programmed with a PC. The sampling time and torque reference values are 133 μsec and 10 N.m, respectively.

Figures 10a and 10b show the operation of the conventional DTC at low (100RPM) and high (1300 RPM) speed. The time delay between the torque controller output and the torque is seen in both the increasing (t_1 and t_2) and decreasing (t_3 and t_4) of the torque. Using the predicted controller as shown in Figs. 10c and 10d eliminates this delay. It can be seen that the torque follows the command of the torque controller immediately. The ripple factor is reduced from 35% in the conventional DTC to 22% in the prediction method at low speed. This improvement is also seen in the high speed behavior of the motor so that the new controller reduces the torque ripple factor from 34% (in conventional DTC) to 16% (in modified DTC).

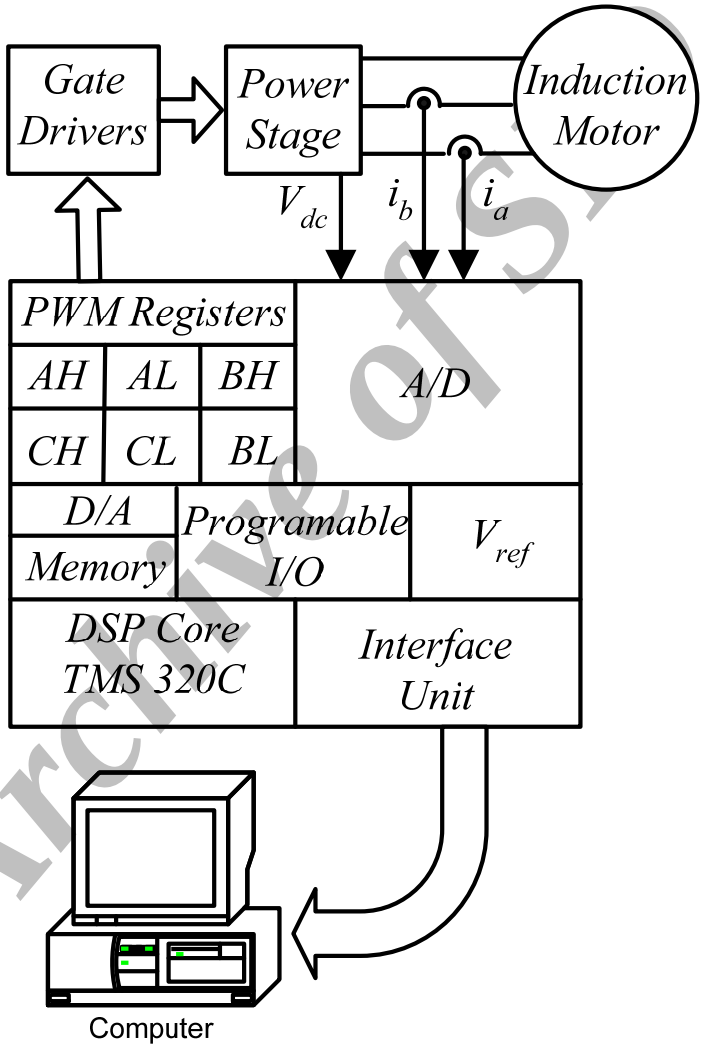

Fig. 9. Experimental setup

Table 3. Characteristics of inverter switches and DSP used in experiments

Parameters of inverter switches	Value	Parameters of DSP	Value
Nominal voltage (V)	600	Clock frequency (MHz)	40
Nominal current (A)	30	Maximum sampling frequency (KHz)	20

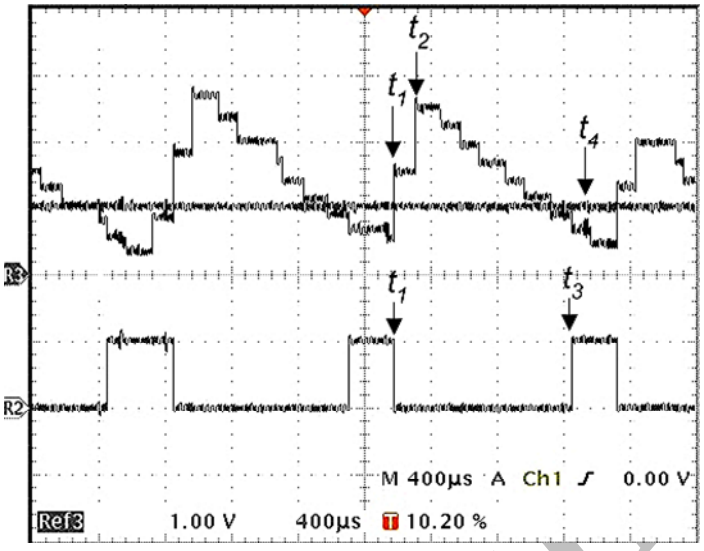

(a)

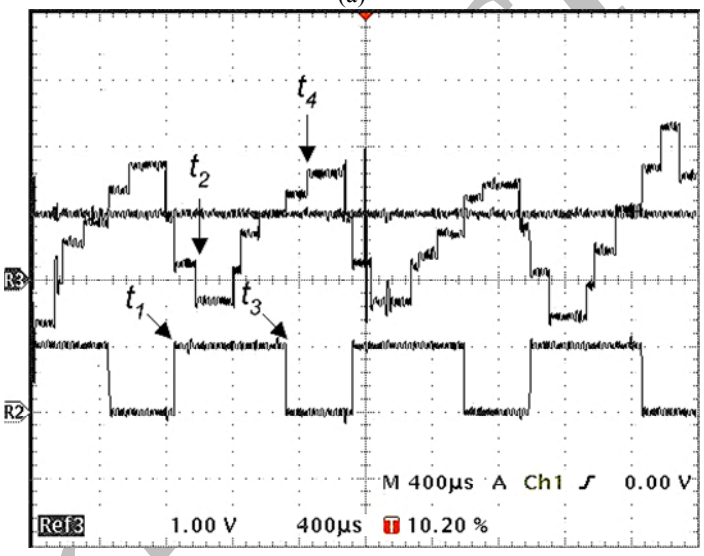

(b)

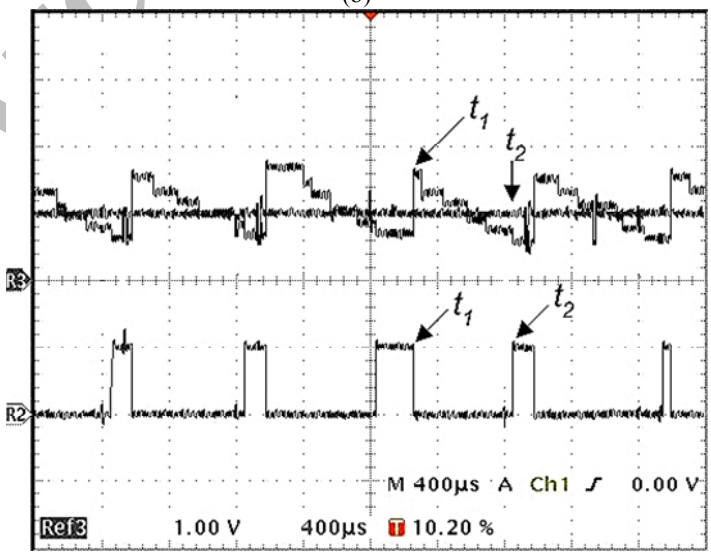

(c)

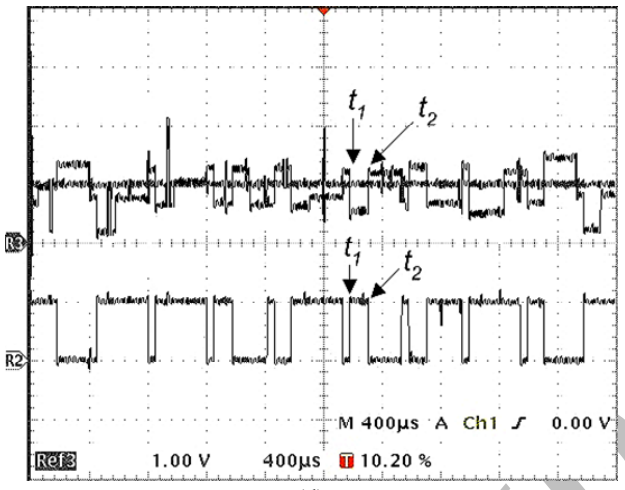

(d)

Fig. 10. Experimental results: Comparison between conventional DTC and proposed method, Up: torque response Down: output of hysteresis torque controller
(a). low speed operation of conventional DTC
(b). high speed operation of conventional DTC
(c). low speed operation of modified DTC
(d). high speed operation of modified DTC

7. CONCLUSIONS

A predictive controller has been proposed which allows the motor to operate with a lower torque ripple than that found in the conventional DTC. This controller predicts the stator current at the end of the sampling interval and calculates the corresponding torque. Thus, application of the voltage vectors is performed online, preventing application of incorrect voltage vectors. The prediction algorithm is based on measurement and is insensitive to the variation of machine parameters. Results show that the new controller decreases the effect of the inherent delay in the control loop of the DTC.

Acknowledgments- The authors would like to thank the Research Department of Sharif University of Technology and France Leading Agency for International Mobility (Egide) for its financial support for the experimental parts of this research.

NOMENCLATURE

Ψ	Flux vector
I	Current vector
U	Voltage vector
T_e	Electromagnetic torque
T_s	Sampling time
~	Superscript for estimated variables
^	Superscript for predicted variables
pp	Pole pair
L	Inductance
ω_m	Motor speed
V_{dc}	Inverter dc-link voltage
R	Winding resistance
$_{s,\ r}$	Subscripts for stator and rotor quantities
$_{d,\ q}$	Subscripts for direct and quadrate axis quantities
$_{av}$	Subscript for averaged quantities
σ	$1-L_m^2/L_sL_r$
L_m	Mutual inductance

REFERENCES

1. Takahashi, I. & Noguchi, T. (1986). A New Quick-Response and High-Efficiency Control Strategy of an Induction Motor. *IEEE Trans. Ind. App.*, *22*(5), 820-827.
2. Schofield, J. R. G., (1995). Direct torque control–DTC. Technical Report, ABB Industrial Systems.
3. Aaltonen, M., Tiitinen, P., Lalu, J. & Heikkila, S. (1995). Direct torque control of AC motor drives. *ABB Review*, *3*(95), 19-24.
4. Mutschler, P. & Flach, E. (1998). Digital Implement of Predictive Direct torque control Algorithms for Induction Motors, *Proc. IEEE Ind. App. Conf.* (444-451).
5. Habetler, T. G., Profumo, F., Pastorelli, M. & Tolbert, M. L. (1992). Direct torque control of induction machines using space vector modulation. *IEEE Trans. Ind. App.*, *28*(5), 1045-1053.
6. Chen, J. & Li, Y. (1999). Virtual vectors based predictive control of torque and flux of induction motor and speed sensorless drives**,** *Proc. IEEE Ind. App. Conf.* (2606-2613).
7. Nillesen, M. E., Duarte, J. L. & Pizzo, A. D. (2000). Direct torque control with application of a predictive pulse width control, *Proc. IEEE Ind. App. Conf.* (1375-1379).
8. Escobar, G., Stankovic, A. M., Galvan, E., Carrasco, J. M. & Ortega, R. (2003). A family of switching control strategies for the reduction of torque ripple in DTC. IEEE *Trans. Control Sys. Tech.*, *11*(6), 933-939.
9. Hu, H. & Li, Y. (2003). Predictive direct torque control strategies of induction motor based on area voltage vectors table, *Proc. IEEE Ind. Elec. Conf.* (2684-2689).
10. Hu, X. & Zhang, L. (1999). A predictive direct torque control scheme for a three-level VSI-fed induction motor drive, *Proc. Power Elec. Machines and Drives Conf.* (334-338).
11. Bolognani, S. & Zigliotto, M. (2002). Full digital predictive hysteresis current control for switching losses minimization in PMSM Drives, *Proc. Power Elec. Machines and Drives Conf.* (61-66).
12. Pacas, M. & Weber, J., (2003). Predictive direct torque control for the PM-synchronous machine, *Proc. IEEE Ind. Elec. Conf.* (1249-1254).
13. Casadei, D., Grandi, G., Serra, G. & Tani, A. (1994). Effects of flux and torque hysteresis band amplitude in direct torque control of induction machines, *Proc. IEEE Ind. Elec. Conf.* (299-305).